Journal of
Nuclear Engineering

MDPI

Article

Powder Metallurgy Produced Aligned Long Tungsten Fiber Reinforced Tungsten Composites

Yiran Mao [1,*], Jan W. Coenen [1,2], Chao Liu [3], Alexis Terra [1], Xiaoyue Tan [4], Johann Riesch [5], Till Höschen [5], Yucheng Wu [4], Christoph Broeckmann [3] and Christian Linsmeier [1]

1 Forschungszentrum Jülich GmbH, Institut für Energie-und Klimaforschung—Plasmaphysik, Partner in the Trilateral Euregio Cluster, 52425 Jülich, Germany
2 Department of Engineering Physics, University of Wisconsin Madison, Madison, WI 53706, USA
3 Institut für Werkstoffanwendungen im Maschinenbau (IWM), RWTH Aachen University, 52062 Aachen, Germany
4 School of Material Science and Engineering, Hefei University of Technology, Hefei 230009, China
5 Max-Planck-Institut für Plasmaphysik, 85748 Garching bei München, Germany
* Correspondence: y.mao@fz-juelich.de

Abstract: For the future fusion reactor, tungsten is the main candidate material as the plasma-facing material. However, considering the high thermal stress during operation, the intrinsic brittleness of tungsten is one of the issues. To overcome the brittleness, tungsten fiber reinforces tungsten composites (W_f/W) developed using extrinsic toughening mechanisms. The powder metallurgy process and chemical vapor deposition process are the two production routes for preparing W_f/W. For the powder metallurgy route, due to technical limitations, previous studies focused on short random distributed fiber-reinforced composites. However, for short random fiber composites, the strength and reinforcement effect are considerably limited compared to aligned continuous fiber composites. In this work, aligned long tungsten fiber reinforced tungsten composites have been first time realized based on powder metallurgy processes, by alternately placing tungsten weaves and tungsten powder layers. The produced W_f/W shows significantly improved mechanical properties compared to pure W and conventional short fiber W_f/W.

Keywords: tungsten fiber reinforced tungsten; field asisted sintering technology; pseudo-ductility; aligned long fiber composites

Citation: Mao, Y.; Coenen, J.W.; Liu, C.; Terra, A.; Tan, X.; Riesch, J.; Höschen, T.; Wu, Y.; Broeckmann, C.; Linsmeier, C. Powder Metallurgy Produced Aligned Long Tungsten Fiber Reinforced Tungsten Composites. *J. Nucl. Eng.* **2022**, *3*, 446–452. https://doi.org/10.3390/jne3040030

Academic Editors: Stjepko Fazinić, Tonči Tadić and Ivančica Bogdanović Radović

Received: 10 October 2022
Accepted: 5 December 2022
Published: 8 December 2022

1. Introduction

As a prominent new energy source, fusion energy offers various advantages, such as a promise of minimal environmental impact and its inherent safety [1]. In addition to plasma physics-related issues, one of the unresolved topics involves material issues related to the first wall and the diverted armor materials, considering the extreme operating condition [2,3]. Tungsten (W) has become the most promising material for this application due to a series of excellent properties such as a high melting point, high thermal conductivity, and a high sputtering threshold [4,5]. However, under fusion conditions with high temperatures and cycled high heat flux, the low fracture toughness of W will lead to the initiation and rapid expansion of cracks in W-based components. Additionally, neutron irradiation will further embrittle the material [6]. Eventually, it can directly affect the safe and efficient operation of fusion devices [7,8]. In order to increase the damage resilience of tungsten material [9], tungsten fiber toughened tungsten composites (W_f/W) are being extensively developed [10–15]. W_f/W does not introduce other metal materials, and its properties are not completely dependent on the intrinsic mechanical properties of the fibers, but also on the toughening mechanism generated by the interaction between the W fibers and the W matrix. Extrinsic toughening mechanisms such as fiber pullout, fiber deformation, crack deflection, and interfacial debonding can consume additional energy during crack propagation. Based on this energy consumption mechanism,

crack propagation can be limited, so that W_f/W composite exhibits "pseudo ductility", and the fracture toughness is greatly improved [16].

W materials are primarily produced by powder metallurgical processes. Field assisted sintering technology (FAST), as a mature powder metallurgy process, is a pressure-assisted sintering synthesis technology using low-voltage pulsed direct current [17,18]. In previous studies [10,19,20], various types of W_f/W have been prepared based on FAST process. Nevertheless, since the introduction of aligned long fibers into a sintering mold is technically challenging, previous studies have mostly used randomly distributed short fibers as reinforcement phases for W_f/W [21]. Compared with the FAST sintered pure W samples, the short fiber W_f/W can already achieve a considerable toughening effect. However, the randomly distributed short fibers have restricted reinforcement efficiency, therefore showing a limited toughening effect compared to aligned long fiber composites prepared by chemical vapor deposition processes [22].

In this work, aligned long fiber W_f/W (L-W_f/W) with dedicated weak interface have been first time prepared by powder metallurgy process. W fiber weaves were used as the toughening phase to prepare L-W_f/W material by the FAST process. The mechanical properties of the prepared samples were tested. The produced L-W_f/W shows significantly improved mechanical properties compared to pure W and conventional short fiber W_f/W.

2. Experiment

2.1. Manufacturing

The production process of L-W_f/W is indicated in Figure 1. The raw materials for the production are W weaves and W powders. The W weaves were woven by the Institute of Textile Technology (ITA), RWTH Aachen University. The warp wires of the weaves have a diameter of 150 µm and a weft wire of 50 µm. The W wires are prepared by a drawn process with an elongated grain structure. Relying on the elongated grain structure, the fibers can give advanced mechanical properties with a tensile strength of ~3000 MPa and a ductile deformation of over 3% [23]. It should be emphasized that the main toughening fibers of the W weaves are unidirectional distributed wrap fibers (with a fiber distance of 200 µm). The weft fibers with a large fiber distance (2 mm) are mainly used to fix the warp fibers. After weaving, the W weaves were cut into circles with a diameter of 39 mm by laser cutting. To establish a fiber/matrix interface, W weaves need to be coated, for which the main candidate interface material is yttrium oxide (yttria) due to its good thermal and chemical stabilities and low activation behavior caused by neutron irradiation. A magnetron sputtering process was used to prepare the coating similar to the procedure reported in [24]. Afterward, the coated W weaves and W powders are alternately placed (20 layers of W weaves and 21 layers of W powders) in the graphite mold (40 mm in diameter) for the FAST process. During the mold packing, ~4 g of W powders were spread between each W weave layer to cover the W weave surface during packing. During the operation, we tried to keep the consistence of spreading W powders for each layer, but sometimes the weaves are not perfectly flat. Additionally, there are operational inaccuracies, as it is manual work. This leads to the inhomogeneity of W weaves in the composites after consolidation, as can be seen in Figure 2. However, this work is only a preliminary approach showing the proof of principle and the production will be optimized later. The consolidation process was performed in a vacuum (<0.1 mbar) at 1850 °C with a pressure of 50 MPa, a holding time of 5 min, and a heating speed of 100 °C/min. A disc shape sample with unidirectional continuous fibers was produced as a result. The relative density of the samples after FAST consolidation is around 91%.

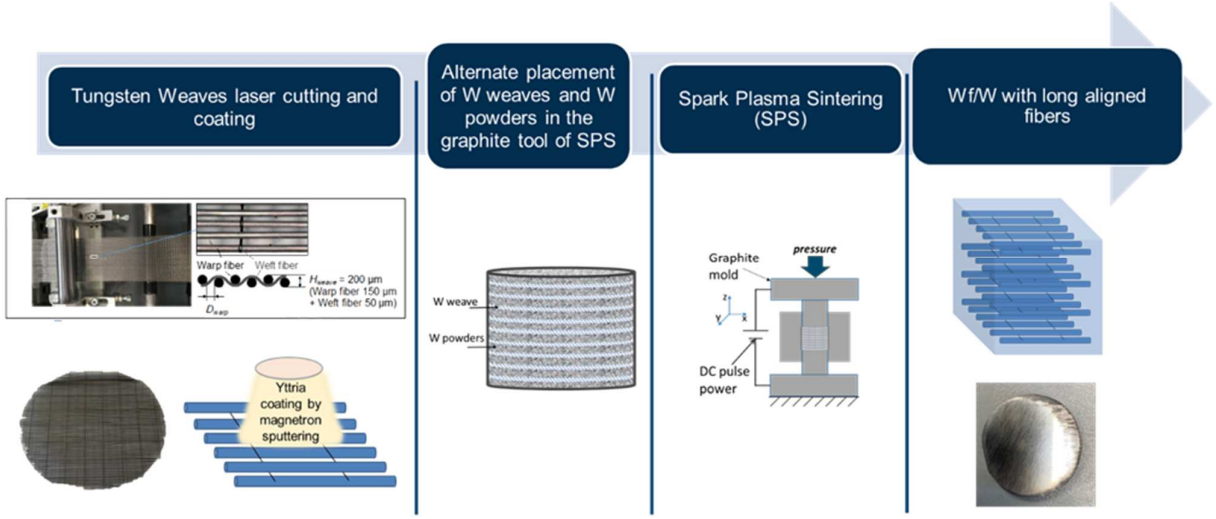

Figure 1. The production procedure of continuous tungsten fiber reinforced tungsten composites.

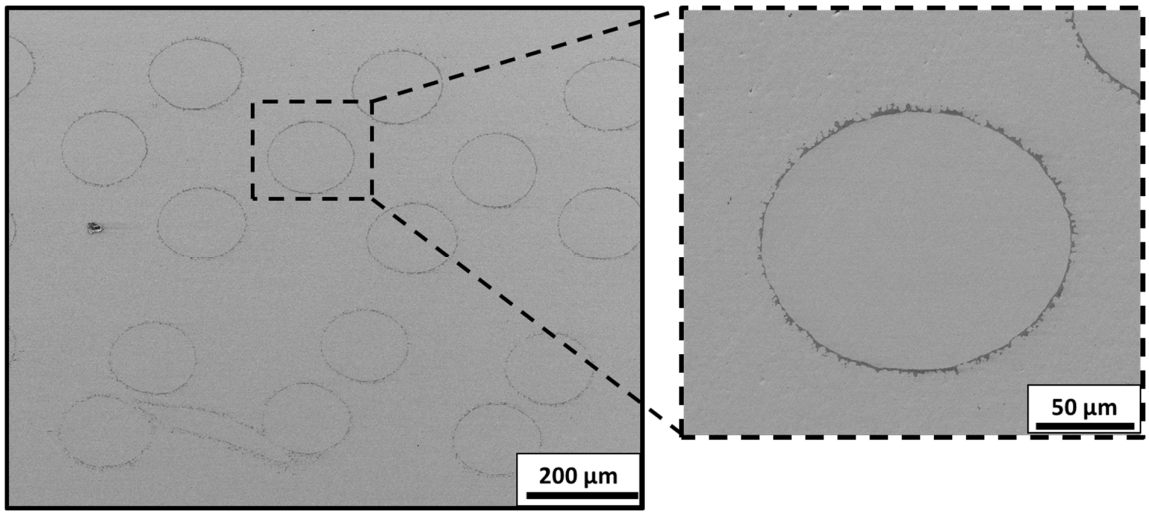

Figure 2. SEM image showing the microstructure of continuous W_f/W.

2.2. Mechanical Characterization

After sintering, to study the fracture behavior, an in-situ 3-point bending test was performed. The 3-point bending samples were manufactured based on the EU standards DIN EN ISO 148-1 and 14556: 2006–2010 [25]. According to this standard, the small-size specimens have the following dimensions (KLST geometry): 27 mm × 3 mm × 4 mm (length × width × thickness), 25 mm span, 1 mm V-notch depth, 0.1 mm notch root radius [26]. The samples were cut by Electrical discharge machining (EDM) without further surface and notch treatment.

The bending tests were performed using a universal testing device (TIRAtest 2820, Nr. R050/01, TIRA GmbH, Schalkau, Germany). During the bending test (1 µm/s testing speed), an optical camera system (DU657M Toshiba, Tokyo, Japan) was used to track the cracking behavior and the absolute sample displacement. The sample displacement in this test is defined as the vertical movement of the sample relative to the reference stage. At the same time, the corresponding force is also recorded. This way a quantitatively measured force-displacement curve can be then determined. Two samples have been tested in total.

Apart from the force-displacement curve, fracture toughness (K_q) can also be calculated based on an ASTM E399 standard [27]. The calculation combines the stable crack

growth length and the corresponding load during the test. More detail regarding the calculation of the fracture toughness can be referred to [20,28].

The 4-point bending tests were performed to measure flexural strength. The 4-point bending test sample dimension is $20 \times 2 \times 2.25\ mm^3$ (length × width × thickness). The tests are applied by using an Instron 3342 universal testing machine (Instron GmbH, Norwood, MA, USA). During the tests, the sample was set on two support pins with a distance of 18 mm. A pressing load from two load pins with a distance of 9 mm was applied in the middle of the sample. The testing speed was 5 µm/s. Three samples have been tested.

3. Results and Discussion

After the sintering process, the microstructure of the W_f/W was analyzed by a Zeiss LEO 982 scanning electron microscope (SEM, Jena, Germany). The typical microstructure is shown in Figure 2. As can be seen from the figure, the fibers are unidirectionally oriented. The fiber volume fraction is around 22%. The yttrium oxide interface is still visible after sintering. However, the layer also becomes partially damaged due to the high temperature and pressure during the sintering process similar to the results in [12].

The typical force-displacement curves of the 3-point bending tests on L-W_f/W are shown in Figure 3, compared to pure W and conventional short fiber W_f/W (data for pure W and conventional short fiber W_f/W is based on [14]). It can be seen that a pseudo ductile behavior can be established by L-W_f/W samples: after a linear-elastic deformation, the slope of the curve changes gradually to negative values after several small load drops; after reaching the maximum force, the samples tend to have a continuous load-decreasing. Even after large deformation (vertical bending displacement >0.3 mm), the sample remains as a whole with a strength above 150 N. Compared to pure W and conventional short fiber W_f/W, L-W_f/W represents a greatly improved pseudo ductility.

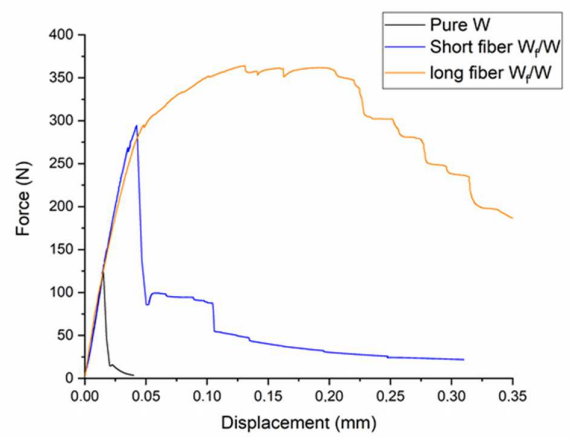

Figure 3. The typical force-displacement curves of the 3-point bending test on KLST samples for long fiber W_f/W in comparison with conventional short fiber W_f/W and pure W [14].

The SEM analysis on the fracture surfaces 3-point bending test is shown in Figure 4. The uneven topology of the surface is an indication of crack deflection. Additionally, fiber/matrix interface debonding and fiber pull-out effects can also be observed. Most of the fibers give a necking effect together with a ductile fracture surface [23]. This shows that the high ductility of the fibers is efficiently utilized.

Based on the measured force-displacement curves and the observed stable cracking length, fracture energy density and fracture toughness can be calculated, as shown in Table 1, together with the typical values for pure W and short fiber W_f/W based on [14]. Additionally, the flexural strength measured by 4-point bending tests is shown here, as well as typical values for pure W and short fiber W_f/W based on [12]. Based on the results in Figure 3 and Table 1, the damage resilience, as well as the strength of the L-W_f/W, is

significantly improved compared to conventional short fiber W_f/W, although the fiber volume fraction is lower (for short fiber W_f/W here, the volume fraction is 30%).

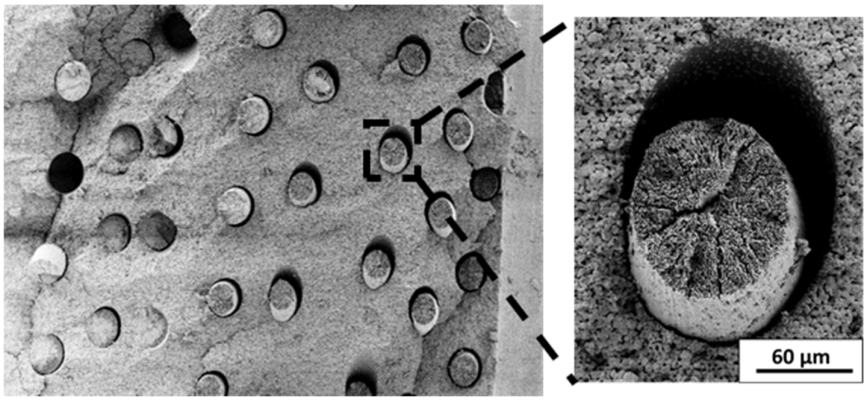

Figure 4. Typical fracture surface after 3-point bending test for long fiber W_f/W.

Table 1. Fracture energy density, fracture toughness, and flexural strength of long fiber W_f/W, compared to conventional short fibre W_f/W, and pure W [12,14].

Samples	Fracture Energy Density (kJ/m^2)	Fracture Toughness, Kq ($MPa\ m^{0.5}$)	Flexural Strength (Mpa)
Pure Tungsten	0.1 ± 0.0	5.5 ± 0.0	381 ± 46
Short fiber W_f/W	1.9 ± 0.7	25.5 ± 7.8	221 ± 17
Long fiber W_f/W	13.2 10.2	82.5 52.6	412 473 600
	11.6 ± 1.5	67.6 ± 15.0	495 ± 78

The improved mechanical properties can be attributed to the following reasons. First of all, due to the random distribution of short fibers, under a given load, there will be a large number of fibers in the W_f/W that are approximately perpendicular to the stress direction. The weak interface between the fiber and matrix will directly bear a large tensile stress, resulting in internal cracking of the material and reducing the strength of the material [29,30]. In addition, the ends of the short fibers will also bear large shear stress, leading to the direct cracking of the interface [31]. The authors' previous research [12] also confirmed that the strength of the randomly distributed short fiber W_f/W material is lower than that of the pure W bulk material prepared by the same powder metallurgy process.

Secondly, the short fibers have the problem of low fiber toughening efficiency. Theoretical studies [32,33] show that the fiber toughening efficiency will increase with the increase of fiber length, and the relationship between fiber toughening efficiency and fiber length can be summarized as [22]:

$$\eta_l = 1 - [\tanh\left(\beta_1 \frac{l}{2}\right)]/\left(\beta_1 \frac{l}{2}\right)$$

where η_l is the reinforcement efficiency, β_1 is the fiber mechanical property term, and l is the fiber aspect ratio.

4. Summary

In this study, aligned long fiber W_f/W with dedicated yttria interface have been for the first time prepared by powder metallurgy process, with significantly improved mechanical properties. Namely, for L-W_f/W, the measured fracture energy density, fracture toughness, and flexural strength are much higher than the conventional short fiber W_f/W and pure W. This is attributed to the much higher reinforcement efficiency of the aligned continuous fiber structure. In the next step, the newly developed L-W_f/W will be further characterized with

fusion-related tests, e.g., plasma erosion, and thermal shock to demonstrate its advanced properties. In addition, efforts will also be put into large-scale production.

Author Contributions: Conceptualization, Y.M., J.W.C. and J.R.; Methodology, Y.M., C.L. (Chao Liu), A.T., X.T. and T.H.; Resources, J.W.C., X.T., Y.W., C.B. and C.L. (Christian Linsmeier); Writing—original draft, Y.M.; Writing—review & editing, Y.M.; Supervision, J.W.C. and C.L. (Christian Linsmeier); Project administration, J.R. and C.L. (Christian Linsmeier). All authors have read and agreed to the published version of the manuscript.

Funding: This work has been carried out within the framework of the EUROfusion Consortium, funded by the European Union via the Euratom Research and Training Programme (Grant Agreement No 101052200—EUROfusion). Views and opinions expressed are however those of the author(s) only and do not necessarily reflect those of the European Union or the European Commission. Neither the European Union nor the European Commission can be held responsible for them.

Data Availability Statement: The data presented in this study are available in [12,14].

Conflicts of Interest: The authors declare no conflict of interest.

References

1. Schumacher, U. Status and problems of fusion reactor development. *Naturwissenschaften* **2001**, *88*, 102–112. [CrossRef] [PubMed]
2. Bolt, H.; Barabash, V.; Krauss, W.; Linke, J.; Neu, R.; Suzuki, S.; Yoshida, N.; Team, A.U. Materials for the plasma-facing compo-nents of fusion reactors. *J. Nucl. Mater.* **2004**, *329–333*, 66–73. [CrossRef]
3. Merola, M.; Loesser, D.; Martin, A.; Chappuis, P.; Mitteau, R.; Komarov, V.; Pitts, R.; Gicquel, S.; Barabash, V.; Giancarli, L.; et al. ITER plasma-facing components. *Fusion Eng. Des.* **2010**, *85*, 2312–2322. [CrossRef]
4. Philipps, V. Tungsten as material for plasma-facing components in fusion devices. *J. Nucl. Mater.* **2011**, *415*, S2–S9. [CrossRef]
5. Coenen, J.W.; Antusch, S.; Aumann, M.; Biel, W.; Du, J.; Engels, J.; Heuer, S.; Houben, A.; Hoeschen, T.; Jasper, B.; et al. Materials for DEMO and reactor applications—Boundary conditions and new concepts. *Phys. Scr.* **2016**, *T167*, 014002. [CrossRef]
6. Bolt, H.; Barabash, V.; Federici, G.; Linke, J.; Loarte, A.; Roth, J.; Sato, K. Plasma facing and high heat flux materials—Needs for ITER and beyond. *J. Nucl. Mater.* **2002**, *307–311*, 43–52. [CrossRef]
7. Pintsuk, G.; Bobin-Vastra, I.; Constans, S.; Gavila, P.; Rödig, M.; Riccardi, B. Qualification and post-mortem characterization of tungsten mock-ups exposed to cyclic high heat flux loading. *Fusion Eng. Des.* **2013**, *88*, 1858–1861. [CrossRef]
8. Huber, A.; Arakcheev, A.; Sergienko, G.; Steudel, I.; Wirtz, M.; Burdakov, A.; Coenen, J.; Kreter, A.; Linke, J.; Mertens, P. Investi-gation of the impact of transient heat loads applied by laser irradiation on ITER-grade tungsten. *Phys. Scr.* **2014**, *T159*, 014005. [CrossRef]
9. Ren, C.; Fang, Z.Z.; Koopman, M.; Butler, B.; Paramore, J.; Middlemas, S. Methods for improving ductility of tungsten—A review. *Int. J. Refract. Met. Hard Mater.* **2018**, *75*, 170–183. [CrossRef]
10. Mao, Y.; Coenen, J.W.; Riesch, J.; Sistla, S.; Almanstötter, J.; Jasper, B.; Terra, A.; Höschen, T.; Gietl, H.; Bram, M.; et al. Development and characterization of powder metallurgically produced discontinuous tungsten fiber reinforced tungsten composites. *Phys. Scr.* **2017**, *T170*, 014005. [CrossRef]
11. Riesch, J.; Buffiere, J.-Y.; Höschen, T.; Di Michiel, M.; Scheel, M.; Linsmeier, C.; You, J.-H. In situ synchrotron tomography estimation of toughening effect by semi-ductile fibre reinforcement in a tungsten-fibre-reinforced tungsten composite system. *Acta Mater.* **2013**, *61*, 7060–7071. [CrossRef]
12. Mao, Y.; Coenen, J.; Riesch, J.; Sistla, S.; Almanstötter, J.; Jasper, B.; Terra, A.; Höschen, T.; Gietl, H.; Linsmeier, C.; et al. Influence of the interface strength on the mechanical properties of discontinuous tungsten fiber-reinforced tungsten composites produced by field assisted sintering technology. *Compos. Part A Appl. Sci. Manuf.* **2018**, *107*, 342–353. [CrossRef]
13. Gietl, H.; Riesch, J.; Coenen, J.; Höschen, T.; Linsmeier, C.; Neu, R. Tensile deformation behavior of tungsten fibre-reinforced tungsten composite specimens in as-fabricated state. *Fusion Eng. Des.* **2017**, *124*, 396–400. [CrossRef]
14. Mao, Y.; Coenen, J.W.; Riesch, J.; Sistla, S.K.; Almanstötter, J.; Reiser, J.; Terra, A.; Chen, C.; Wu, Y.; Raumann, L.; et al. Fracture behavior of random distributed short tungsten fiber-reinforced tungsten composites. *Nucl. Fusion* **2019**, *59*, 086034. [CrossRef]
15. Mao, Y.; Coenen, J.W.; Terra, A.; Gao, L.; Kreter, A.; Wirtz, M.; Liu, C.; Chen, C.; Riesch, J.; Wu, Y.; et al. Demonstrating tungsten fiber-reinforced porous-matrix tungsten composites for future fusion application. *Nucl. Fusion* **2022**, *62*, 106029. [CrossRef]
16. Riesch, J.; Han, Y.; Almanstötter, J.; Coenen, J.W.; Höschen, T.; Jasper, B.; Zhao, P.; Linsmeier, C.; Neu, R. Development of tungsten fibre-reinforced tungsten composites towards their use in DEMO—Potassium doped tungsten wire. *Phys. Scr.* **2016**, *T167*, 014006. [CrossRef]
17. Mao, Y.; Coenen, J.W.; Riesch, J.; Sistla, S.; Chen, C.; Wu, Y.; Raumann, L.; Neu, R.; Linsmeier, C.; Broeckmann, C. Spark Plasma Sintering Produced W-Fiber-Reinforced Tungsten Composites. In *Spark Plasma Sintering of Materials: Advances in Processing and Applications*; Cavaliere, P., Ed.; Springer International Publishing: Cham, Switzerland, 2019; pp. 239–261.

18. Guillon, O.; Gonzalez-Julian, J.; Dargatz, B.; Kessel, T.; Schierning, G.; Räthel, J.; Herrmann, M. Field-Assisted Sintering Technology/Spark Plasma Sintering: Mechanisms, Materials, and Technology Developments. *Adv. Eng. Mater.* **2004**, *16*, 830–849. [CrossRef]
19. Jiang, Y.; Zhang, L.; Fang, Q.; Zhang, T.; Wang, X.; Hao, T.; Liu, C. Toughness enhancement of tungsten reinforced with short tungsten fibres. *Mater. Sci. Eng. A* **2017**, *690*, 208–213. [CrossRef]
20. Mao, Y.; Coenen, J.; Sistla, S.; Liu, C.; Terra, A.; Tan, X.; Riesch, J.; Hoeschen, T.; Wu, Y.; Broeckmann, C.; et al. Design of tungsten fiber-reinforced tungsten composites with porous matrix. *Mater. Sci. Eng. A* **2021**, *817*, 141361. [CrossRef]
21. Mao, Y.; Coenen, J.W.; Riesch, J.; Sistla, S.; Almanstötter, J.; Terra, A.; Chen, C.; Wu, Y.; Raumann, L.; Höschen, T.; et al. Fiber Volume Fraction Influence on Randomly Distributed Short Fiber Tungsten Fiber-Reinforced Tungsten Composites. *Adv. Eng. Mater.* **2020**, *22*, 1901242. [CrossRef]
22. Laws, V. The efficiency of fibrous reinforcement of brittle matrices. *J. Phys. D Appl. Phys.* **1971**, *4*, 1737–1746. [CrossRef]
23. Riesch, J.; Almanstötter, J.; Coenen, J.W.; Fuhr, M.; Gietl, H.; Han, Y.; Höschen, T.; Linsmeier, C.; Travitzky, N.; Zhao, P.; et al. Properties of drawn W wire used as high performance fibre in tungsten fibre-reinforced tungsten composite. *IOP Conf. Ser. Mater. Sci. Eng.* **2016**, *139*, 012043. [CrossRef]
24. Mao, Y.; Engels, J.; Houben, A.; Rasinski, M.; Steffens, J.; Terra, A.; Linsmeier, C.; Coenen, J. The influence of annealing on yttrium oxide thin film deposited by reactive magnetron sputtering: Process and microstructure. *Nucl. Mater. Energy* **2017**, *10*, 1–8. [CrossRef]
25. *DIN 50115*; Notched Bar Impact Testing of Metallic Materials Using Test Pieces other than ISO Test Pieces. Deutsches Institut fur Normung: Berlin, Germany, 1991.
26. Rieth, M.; Hoffmann, A. Influence of microstructure and notch fabrication on impact bending properties of tungsten materials. *Int. J. Refract. Met. Hard Mater.* **2010**, *28*, 679–686. [CrossRef]
27. *ASTM E399-17*; Standard Test Method for Linear-Elastic Plane-Strain Fracture Toughness K_{Ic} of Metallic Materials. ASTM International: West Conshohocken, PA, USA, 2017.
28. Gietl, H.; Olbrich, S.; Riesch, J.; Holzner, G.; Höschen, T.; Coenen, J.; Neu, R. Estimation of the fracture toughness of tungsten fibre-reinforced tungsten composites. *Eng. Fract. Mech.* **2020**, *232*, 107011. [CrossRef]
29. Meraghni, F.; Blakeman, C.J.; Benzeggagh, M.L. Effect of interfacial decohesion on stiffness reduction in a random discontin-uous-fibre composite containing matrix microcracks. *Compos. Sci. Technol.* **1996**, *56*, 541–555. [CrossRef]
30. Zhang, H.; Zhang, Z.; Breidt, C. Comparison of short carbon fibre surface treatments on epoxy composites: I. Enhancement of the mechanical properties. *Compos. Sci. Technol.* **2004**, *64*, 2021–2029. [CrossRef]
31. Hu, X.; Fang, J.; Xu, F.; Dong, B.; Xiao, Y.; Wang, L. Real internal microstructure based key mechanism analysis on the mi-cro-damage process of short fibre-reinforced composites. *Sci. Rep.* **2016**, *6*, 34761. [CrossRef]
32. Nguyen, B.N.; Bapanapalli, S.K.; Holbery, J.D.; Smith, M.T.; Kunc, V.; Frame, B.J.; Phelps, J.H.; Tucker, C.L., III. Fiber Length and Orientation in Long-Fiber Injection-Molded Thermoplastics—Part I: Modeling of Microstructure and Elastic Properties. *J. Compos. Mater.* **2008**, *42*, 1003–1029. [CrossRef]
33. Gray, R.J. Analysis of the effect of embedded fibre length on fibre debonding and pull-out from an elastic matrix. *J. Mater. Sci.* **1984**, *19*, 861–870. [CrossRef]